OPTOELECTRONICS AND ADVANCED MATERIALS – RAPID COMMUNICATIONS Vol. 1, No. 12, December 2007, p. 683 - 688

Post annealing effect on SnO_2 thin films grown by thermal evaporation technique

A. SHARMA*, D. PRAKAH[a], K. D. VERMA
Material Science Laboratory, Department of Physics, S.V.College, Aligarh (U.P.) India
[a]Department of Computer Science & Engineering, C-DAC, Noida, U.P., India

Nanocrystalline tin oxide thin films were prepared by thermal evaporation technique. The grain sizes, crystallization process and morphology were investigated by x-ray diffraction (XRD) and Atomic Force Microscopy (AFM). Both optical band gap and transmittance were enhanced after heat treatment. All IR modes measured by Fourier Transform Infrared Microscopy (FTIR) spectrometer were assigned. The FTIR spectra show an increase in the intensity of the E_u mode (606.75 cm^{-1}) after post annealing, which indicates fine crystallization of SnO_2 grains. Thermal treatment induced defects enhance the diffusion of atoms leading to uniformity in size of grains. But the grains were found to be elongated and larger in size, in case of SnO_2 films on quartz substrate deposited. The role of substrate on thermal treatment induced grain growth process is discussed.

(Received November 22, 2007; accepted November 28, 2007)

Keywords: Nanocrystalline, Thin films, Grain growth process, Diffusion, AFM, XRD, FTIR etc.

1. Introduction

Low dimensional inorganic nanostructured materials have evoked much interest owing to their possible applications in technological fields. The preparation of the nanosized crystallites with different morphologies provides an opportunity to explore the possible changes in their physical and chemical features with size and shape. Since for any technological application, thin films with good electrical and optical properties with suitable substrates are required. Therefore, fabrication of thin films for metal oxide compounds hold final key to any of its property. The film growth of these compounds is being carried out for last two decades [1-3] and the optimization of the growth parameters has been benefited from the studies of high quality thin films. Several growth techniques have been employed in this context such as sputtering [4], e-beam evaporation [5-6], sol-gel methods [7-8], and pulsed laser deposition [9] etc. Films deposited by these techniques are typically polycrystalline, retaining the crystal structure of the bulk material. Thermal evaporation is also widely used and well known technique generally, to deposit thin films with smoother surface than other techniques with less or no damage at the substrate interface. Sufficiently conducting and transparent thin films for device application are obtained by thermal evaporation process with controlled conditions and post annealing [6].

A large lattice mismatch between the substrate and film may cause compressive/tensile strains in the film which may lead to concomitant change in crystalline nature (in plane alignment) and affect the bond angle and bond length of the unit cell. This brings out the limitation in the choice of the substrate for thin film deposition. To relieve internal stresses, refine the structure and improve cold working properties of the materials thermal annealing process is used. If annealing is allowed to high temperatures once recrystallization process has been completed, grain growth will occur, in which the microstructure starts to coarsen and may cause the material to have less than satisfactory mechanical properties. However, the annealing effect on grain growth process in different substrate grown metal oxide thin films has not been elucidated clearly.

Only in the past few years have a few papers reported [9-10] the use of XRD for more detailed studies of the lattice distortion in thin films and change in their microstructures with annealing temperature. On the other hand, UV-visible spectroscopy is widely used to reveal the variation in optical band gap, transmittance/absorbance and also provide information about the crystallinity of the nanocrystalline transparent metal oxide semiconductors [4, 11]. XRD and UV-visible spectroscopy together with AFM and FTIR measurements might enhance our understanding of the grain growth process and post annealing effect on physical properties and chemical composition of different substrate grown thin films.

Tin oxide (SnO_2) is an n-type semiconductor which possess perfect physical properties, super chemical stability and low cost. All these properties have stimulated its applications in active and passive electronic devices. Additionally, the material shows high variation of the electrical resistance in the presence of oxidizing and reducing gases. Thin SnO_2 films exhibit high optical transparency in the visible region. These advantageous properties are used for gas sensor application [7, 12]. In nanocrystalline SnO_2, the above properties have been extensively explored [13-14], and this material will find wide applications in microelectronics, sensors and compound function ceramics. The attempt to improve properties of SnO_2 thin films largely relies on understanding the role of substrate in grain growth process

and post annealing effects. In the present study, nanocrystalline SnO_2 thin films are deposited on both crystalline and amorphous substrates using thermal evaporation technique to understand the role of substrate in the growth of SnO_2 grains. These films were annealed in oxygen environment to study thermal treatment induced changes in structural properties, optical band gap, absorbance, and chemical composition of the SnO_2.

2. Experimental details

First, tin oxide powder was synthesized by hydrothermal process and then thin films were deposited on silicon (Si) and quartz substrates. The powder was evaporated (in the form of sintered pallets) by employing 225A current to the Mo boat. The distance from source to substrate and quartz crystal (thickness monitor) was 15 cm and the deposition rate was 0.25–1 nm/s. The vacuum before and during deposition was 5×10^{-7} torr and 6×10^{-5} torr, respectively. The thickness of the films was about to 200 nm. These films were annealed for 3 hours in oxygen flow at different temperatures. The sample codes and annealing temperatures of different samples are shown in the Table 1. XRD measurements were carried out using Bruker D8 advanced diffractometer for determining crystallinity and orientation of SnO_2 powder as well as thin films using CuKα radiation (λ = 1.540Å). Morphology of the films was analyzed by AFM in tapping mode by using digital Nanoscope IIIa SPM. Optical absorption spectra were recorded with the conventional two beam method using Hitachi UV-3300, UV-VIS spectrometer. The O-Sn-O bonding of SnO_2 thin films were studied by FTIR spectroscopy by using Thermal Nicolet NEXUS 670 FT-IR spectrometer.

Table 1. Sample coeds with annealing temperatures with average grain sizes of different samples.

Samples	Powder	Si substrate deposited				Quartz substrate deposited			
		As-deposited	200 °C annealed	500 °C annealed	900 °C annealed	As-deposited	200 °C annealed	500 °C annealed	900 °C annealed
Code	P	S1	S2	S3	S4	Q1	Q2	Q3	Q4
Average Grain-Size	34 nm	-	-	11.74 (nm)	12.08 (nm)	-	-	13.03 (nm)	13.97 (nm)

3. Results and discussion

Tin oxide has a tetragonal rutile crystalline structure (known in its mineral form as cassiterite) with point group D_{4h}^{14} and space group P42/mnm. The unit cell consists of two metal atoms and four oxygen atoms. Each metal atom is situated amidst six oxygen atoms which approximately form the corners of a regular octahedron. Oxygen atoms are surrounded by three tin atoms which approximate the corners of an equilateral triangle. The lattice parameters of SnO_2 are, a = 4.7382(4) Å and c = 3.1871(1) Å [15]. Fig. 1 shows XRD spectra of different samples. The sample P shows all the peaks correspond to the rutile phase of SnO_2 indicating high quality of powder. While samples S1and Q1 do not show any peak of rutile phase and exhibit amorphous nature. The S2 and Q2 also exhibit same behavior in XRD spectra as samples S1 and Q1 show, because the low temperature annealing can only lead to a relaxation in the interface structure, it cannot dispel the local lattice disorders or change the internal structure of the grains, so there is no apparent change in the crystallinity of the 200 ^{0}C annealed thin films. Rutile SnO_2 diffraction peaks appear for samples S3, S4, Q3 and Q4 with a preferential growth in (110) orientation, because the (110) surface presents minimum surface energy in comparison to other surfaces [16]. This suggests that growth in the (110) direction will result in particles with higher aspect ratio than the growth in the other directions or even in the substrate direction. The average grain sizes were calculated from XRD patterns, by using Scherrer formula $D = 0.9\lambda/\beta \cos\theta$, where D is the diameter of the grains, λ is the wavelength of the x-rays and β is the full width half maximum (FWHM) of the diffraction peaks. Thus, the calculated grain sizes for different samples are shown in Table 1. The grain sizes observed in the AFM micrographs are larger than those estimated from the XRD data, indicating significant agglomeration of the grains. It is known that, for the tetragonal structure the lattice parameters can be calculated by

$$d_{(hkl)} = \frac{1}{\sqrt{\frac{h^2+k^2}{a^2}+\frac{l^2}{c^2}}} \quad (1)$$

Where, h, k, and l are all integers, (hkl) is the lattice plane and a and c are lattice constants. For a real crystal, the calculated values of a and c are the same for different crystal planes. However, the presence of a large number of defects (vacant lattice sites and local lattice disorders) may lead to obvious reduction of intensities (or even disappearance) of XRD peaks of some lattice planes [e.g., the lattice plane (111) and (220) were absent in S3 and Q3 samples while (111), (220) and (002) peaks were found to be absent in Q3, and Q4 samples]. Therefore, these results imply destroyed periodicity in some crystal planes and a significant distortion of the rutile lattice. We

have compared $d_{(hkl)}$ values and calculated the lattice parameters (a and c) of different samples by using equation (1), are shown in the Table 2 and 3, respectively. From the Table 3, we can see that there is an increase in a and a little decrease in c for the annealed samples. This implies that the films may contain large number of defects and local lattice disorders, which lead to change in the lattice parameters and responsible for the poor crystallinity of the SnO_2 thin films. Besides this, as discussed earlier, presence of strains due to the lattice mismatch between the substrate and thin film largely affect the crystalline nature of the films. The percentage lattice mismatch (σ) between the film and substrate can evaluated as

$$\sigma = \frac{(a_{substrate} - a_{film})}{a_{substrate}} \times 100 \qquad (2)$$

where a is the lattice parameter. The positive value of σ corresponds to the tensile strain (the cell is elongated in the films plane and compressed along the out of plane growth direction). Whereas the negative value of σ corresponds to the compressive stress (the cell is compressed in the films plane and elongated along the out of plane growth direction). The percentage lattice mismatch calculated by using equation (2) were found to be around 12.71% and 3.56% in the Si and quartz substrate grown SnO_2 films, respectively, which may responsible for low intensity of diffraction peaks in XRD measurement. AFM micrographs of samples S3 and Q3 are shown in the Fig. 2a and 2b, respectively. The figures show the SnO_2 grains are relatively well separated. Besides well separated grains, SnO_2 thin films also contain some agglomeration lumps. This may be due to the diffusion process, where particles undergo multiple collisions leading to coagulation and agglomeration and growth in size. The rate at which agglomeration occurs depends primarily on number of particles (initial concentration) and their mobility [17]. Agglomeration rate (R_f) is given by $R_f = k_f n_0^2$, where n_0 is initial concentration and $k_f = 4k_B T / 3\eta$, k_B is the Boltzmann constant, T is temperature, and η is viscosity of the medium. As the particles size decreases towards the molecular level, their behavior is more like vapor. The kinetic behavior of nanograins follows the basic low of gaseous diffusion. Due to increase in the size of particles and decrease in their initial concentration in annealed thin films, the rate of agglomeration process decreases substantially leading to the formation of narrow size distribution of grains. Thus, the results of imaging studies support the results of structural studies.

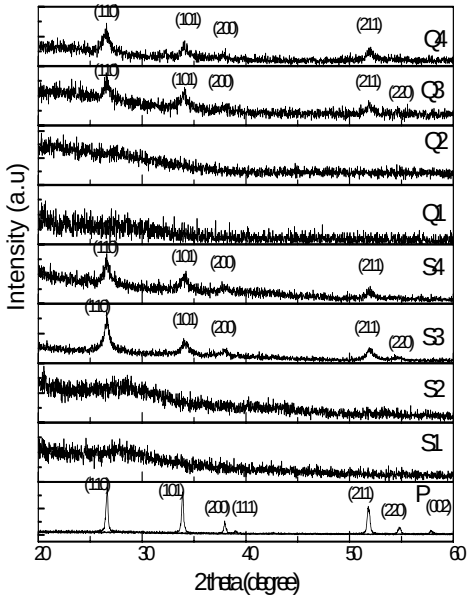

Fig. 1. XRD spectra of SnO_2 powder and thin film samples.

Table 2. Comparison of $d_{(hkl)}$ values of different samples.

$d_{(hkl)}$	Ref [15] (Å)	P (Å)	S3 (Å)	S4 (Å)	Q3 (Å)	Q4 (Å)
(110)	3.3470	3.3477	3.3486	3.3482	3.3555	3.3523
(101)	2.6427	2.6433	2.6331	2.6169	2.6273	2.6261
(200)	2.3690	2.3705	2.3567	2.2841	2.3712	2.3647
(111)	2.3094	2.3104				
(210)	2.1189	2.1186				
(211)	1.7641	1.7648	1.7601	1.7579	1.7622	1.7538
(220)	1.6750	1.6757	1.68751			
(002)	1.5934	1.5946				
(310)	1.4984	1.4980				
(221)	1.4829					
(112)	1.4392	1.4312				
(301)	1.4155	1.4157				

Table 3. Lattice parameters and change in lattice parameters for different samples.

Lattice parameters	Ref [15] (Å)	P (Å)	S3 (Å)	S4 (Å)	Q3 (Å)	Q4 (Å)
a_{110}	4.7333	4.7343	4.7356	4.7350	4.7453	4.7408
a_{200}	4.7380	4.7410	4.7134	4.5682	4.7424	4.7294
Δa	-0.0047	-0.0067	0.0222	0.1668	0.0029	0.0114
$c_{101\text{-}110}$	3.1856	3.1862	3.1678	3.1399	3.1549	3.1541
$c_{101\text{-}200}$	3.1839	3.1842	3.1749	3.1925	3.1555	3.1575
Δc	0.0017	0.0020	-0.0071	-0.0526	-0.0006	-0.0034

During the thermal annealing process, a large number of point defects like oxygen vacancies are expected to generate in the SnO_2 films as well as in the substrate. As the total fraction of surface atoms increases drastically in the nanostructures, an increasing number of metal oxygen bonds would become weaker in these systems, which may facilitate the desorption of the oxygen-ions from the lattice, thus creating more oxygen-ion vacancies. It is assumed that the defects are generated through out the grains and they migrate to grain boundaries where they affect the mobility of the grain boundaries. SnO_2 grains are expected to be nucleated around these large numbers of vacancies and can grow uniformly with time. As nucleation and growth process are separated, uniform size distribution of grains occurs. But the number of vacancies generated in the Si substrate grown films are less compared to that quartz substrate grown films. The reduced number of defects generated in the Si substrate grown films lead to less number of nucleation centers which are quite separated from each other. Besides this, the thermal diffusivity of quartz is quite less compared to that of Si, so the heat generated in case of Si substrate grown SnO_2 films get dissipated quite quicker than that of dissipated in case of quartz grown films. Due to high diffusivity the spatial confinement of heat is less in case of Si grown films thus leading to smaller size of grains after thermal annealing, compared to that of quartz grown films. When films annealed at 900 ^oC temperature (samples S4 and Q4) the vacancies assemble and form vacancy clusters at the interface of the grains which leads to local state of interface, as a result the crystallinity of these films becomes worse, as we observed in our XRD measurements. The experimental results show that crystallization and grain growth are strongly related in SnO_2 thin films suggesting a common mechanism controlling all of them.

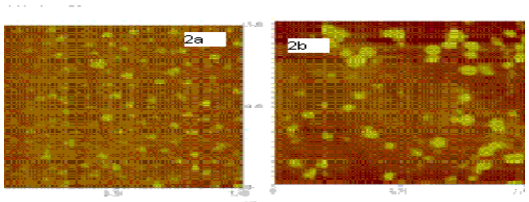

Fig. 2. AFM micrographs of S3 and Q3 samples.

To investigate the effect of annealing temperature on optical absorption and band gap of the SnO_2 thin films, UV-Vis spectra of Q1, Q2, Q3, and Q4 samples were employed, which are shown in the Fig. 3. The Q1and Q2 samples have a significant, continuous absorption in the visible range of the light, demonstrating the presence of a noticeable amount of metallic tin and considerable amount of defects in the films. The metallic tin may be incorporated in the films as droplets or as coherent domains of metallic tin with tin oxide. The absorbance shows strong temperature dependence. It is sufficient in case of Q1 and Q2 samples and decreases with further increasing in the annealing temperatures. The decrease in the absorbance in the annealed SnO_2 films is likely to be related, to the increase in the SnO_2 to Sn ratio. If the size of grains is small enough, the higher surface to volume ratio incorporates various surface related defects in the grains. This causes a broadening of the absorption spectra at the absorption edge. Moreover, an inhomogeneous size distribution of the grains also contributes different degrees of absorption, rendering a broadening of the spectra at the absorption edge; this may be the reason for broadening of the absorption edge in case of Q1, and Q2 samples. The band edges of SnO_2 thin films become sharper for Q3 and Q4 samples. The sharp rise of the spectra at the absorption edge of Q3 and Q4 samples demonstrates that the grains are sufficiently large in size and homogeneously distributed in the films. From the optical absorption spectra the band gap of SnO_2 films were determined using the Tauc's procedure of plotting $(\alpha h\nu)^2$ versus $h\nu$, where α is the absorption coefficient and $h\nu$ in the photon energy (inset Fig. 3). The band gap was found to be 2.70eV, 2.76eV, 2.89eV, and 3.71eV for Q1, Q2, Q3, and Q4 samples, respectively. The small band gap in the as-deposited and low temperature annealed films may be attributed to the energy levels in the intrinsic band gap of SnO_2 due to the defects such as tin ions at interstitial sites and oxygen vacancies. The increase in the band gap energy upon increasing the post annealing temperature is due to the decrease in the amount of defects and/or

increase in the formation of nanocrystalline grains in the films, as we observed in XRD and AFM studies.

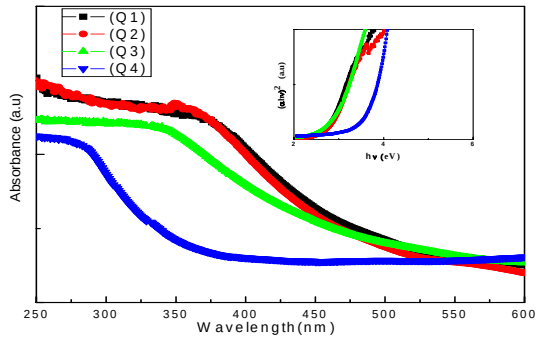

Fig. 3. Absorbance spectra of snO_2 thin films (Inset shows the band gap of the different samples).

To study the effect of the annealing temperature on the chemical bonding of SnO_2, the room temperature FTIR spectra of Si substrate grown films were recorded in the range of 250-4000 cm^{-1} in transmission mode, which are shown in the Fig. 4. The strong IR bands at 2920.31 cm^{-1}, 2848.94 cm^{-1}, and 1041.07 cm^{-1} were assigned as the vibrational mode of (O-H) group and the other bands at 1368.88 cm^{-1}, 1041.07 cm^{-1} and 803.20 cm^{-1} were attributed to metal hydroxide networking (Si-OH or Sn-OH) in the films. In case of sample S4, the bands at 1368.88 cm^{-1}, 1041.07 cm^{-1} and 803.20 cm^{-1} were removed completely and the intensity of the bands at 2920.31 cm^{-1}, 2848.94 cm^{-1}, and 1041.07 cm^{-1} found to be decrease, which indicate that the adsorbed water was taken off from the samples by heat treatment. The silicon and tin hydroxide band disappeared completely after heat treatment because of the dehydration/condensation reaction, resulting formation of Si-O-Si/O-Si-O and O-Sn-O bonding from the metal hydroxide network. The band at 1118.44 cm^{-1} appeared in all samples was assigned to the vibrational mode of Si-O-Si/O-Si-O groups [18]. For bulk SnO_2 crystals with rutile structure, there are two active IR modes at 465 cm^{-1} (A_{2u}) and 605 cm^{-1} (E_u) [19]. The shape of the FTIR spectra may be differ from those for bulk because both the particle size and shape have a great influence on IR spectra [20]. In the present work, Fig. 4 shows a strong band at 606.75 cm^{-1} with a small band at 465.80 cm^{-1}, that in an evidence of the presence of SnO_2 grains in all samples. When the annealing temperature reaches to 900 ^oC the band at 606.75 cm^{-1} become sharper and the band at 465.80 cm^{-1} become week. The 606 cm^{-1} mode (E_u) normally exists in bulk [19]. The appearance of this mode indicates that after heat treatment smaller grains become bigger and the amorphous phases transform into crystalline phase. These results are in good agreement with our structural, imaging and optical absorbance studies.

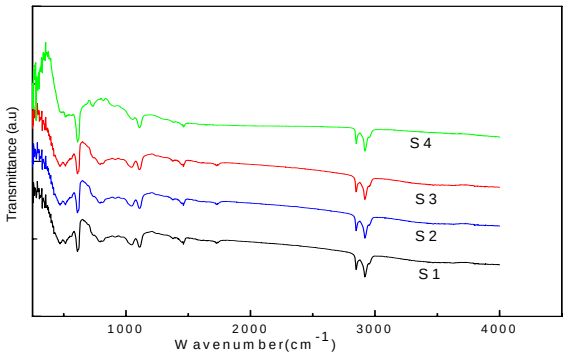

Fig. 4. FTIR spectra of SnO_2 thin films (Deposited on Si substrate).

4. Conclusions

SnO_2 thin films were successfully deposited on Si and Quart substrates by thermal evaporation technique. The crystallinity, band gap, optical absorbance, and chemical bonding of SnO_2 thin films show strong temperature dependence. The grain growth in both substrate grown films is strongly related to the diffusion process and presence of thermal treatment induced defects. Studies on thermal annealing enhanced grain boundary motion may lead to further insight into the relationship between the structure and the properties of grain boundaries and other interfaces.

Acknowledgements

The authors are thankful to material science group, Inter University Accelerator Center (IUAC), New Delhi for providing experimental facilities. One of the authors (A. Sharma) is grateful to the IUAC for providing financial support under the UFUP project.

References

[1] K. B. Sundaram, G. K. Bhagavat, J. Phys. D: Appl. Phys. **16**, 69 (1983).
[2] I. A. Qazi, P. Akhater, A. Mufti, J. Phys. D: Appl. Phys. **24**, 81 (1991).
[3] T. J. Stanimirova, P. A. Atansov, I. G. Dimitrov, A. O. Dikovska, J. Optoelectron. Adv. Mater. **7**, 1335 (2005).
[4] T. Mohanty, Y. Batra, A. Tripathi, D. Kanjilal, J. Nanoscience and Nanotechnology **7**, 2036 (2007).
[5] K. S. Shamala, L. C. S. Murthy, K. Narasimharao, Bull. Mater. Sci. **27**, 295 (2004).
[6] D. C. Agarwal, R. S. Chauhan, Amit Kumar, D. Kabiraj, F. Singh, S. A. Khan, D. K. Avasthi, M. Kumar, J. Ghatak, P. V. Satyam, J. Appl. Phys. **99**, 123105 (2006).
[7] Qun Dong, Huilan Su, Di Zhang, Fangying Zhang, Nanotechnology **17**, 3968 (2006).
[8] Sunita Mishra, C. Ghanshyam, Nathi Ram, Satinder

Singh, R. P. Bajpai, R. K. Bedi, Bull. Mater. Sci **25**, 231 (2003).
[9] Z. W. Chen, J. K. L. Lai, C. H. Shek, Phys. Rev. B **70**, 165314 (2004).
[10] K. N. Yu, Yonghong Xiong, Yolong Liu, Caoshui, Phys. Rev. B **55**, 2666 (1997).
[11] Soumen Das, Soumitra Kar, Subhadra Choudhuri, J. Appl. Phys. **99**, 114303 (2006).
[12] Chi- Hwan Han, Sang-Do Han, S. P. Khatkar, Sensors **6**, 492 (2006).
[13] E. Comini, G. Faglia, G. Sberveglieri, Zhengwei Pan, Zhong L. Wang, Appl. Phys. Lett. **81**, 1869 (2002).
[14] T. P. Hulser, H. Wiggers, F. E. Kruis, A. Lorke, Sensors and Actuators B, **109**, 13 (2005).
[15] G. Mc Carthy, J. Welton, Powder Diffr, **4**, 156 (1989).
[16] M. Batzill, U. Diebold, Prog. Sur. Sci. **79**, 47 (2005).
[17] L. B. Kiss, J. Soderlund, G. A. Niklasson, C. G. Grangvist, Nanotechnology **10**, 25 (1999).
[18] Naoto Shirahata, Woosuck Shin, Norimitsu Murayama, Yoshifake Masuda, Kunihito Koomoto, J. Ceramic Society of Japan, **112**, S 562 (2004).
[19] R. Summit, J. Appl. Phys. **39**, 3726 (1968).
[20] J. X. Zhou, M. S. Zhang, J. M. Hong, J. L. Fang, Z. Yin, Appl. Phys. A, **81**, 177 (2005).

*Corresponding author: adityaiuac@gmail.com